APPENDIX B

Plant Models

B.1 Introduction

This appendix contains descriptions and mathematical models of most of the plants used as Examples and/or Problems in the text. Table B.1 lists them in order of the degree of the characteristic polynomial.

B.2 Ground Vehicles and Robots

B.2.1 Lateral Intercept and Rendezvous

Figure B.1 shows a pursuer with a closing velocity V relative to a nonmaneuvering target, parallel to an initial line of sight (ILOS) to the target, and a relative velocity $v(t)$ perpendicular to the ILOS. The current LOS makes an angle σ with the ILOS; hence

$$\sigma \approx \frac{y}{R},$$

where R is the range-to-go and $T = -R/\dot{R}$ is the time-to-go. The relative acceleration and position perpendicular to the ILOS are $a(t)$ and $y(t)$, so the equations of motion are

$$\dot{y} = v, \qquad \dot{v} = a.$$

The rendezvous performance index is

$$J = \frac{1}{2}\{s_y[y(t_f)]^2 + s_v[v(t_f)]^2\} + \frac{1}{2}\int_0^{t_f} a^2\, dt,$$

where $y(0) = 0$, $v(0) = v_0$, and t_f is given. For the intercept put $s_v = 0$.

TABLE B.1 PLANT MODELS

Description	Characteristic Polynomial	Applications
Single Integ. (SI)	s	1-D DR nav., 1-D survey route
First-order Lag	$s + p$	Temp. change, vehicle/engine/motor velocity
Double integrator (DI)	s^2	Vehicle lat. motion, lat. intercept/rendezvous S/C Pitch, 2-D DR nav., 2-D survey route
Integrator lag	$s(s + p)$	Vehicle/engine/motor position, Reservoir Volume, Brownian Motion
Stable mode	$s^2 + \omega^2$	Pendulum, spring–mass, orbital gyrocompass
Unstable mode	$s^2 - \eta^2$	Bicycle, inverted pendulum
Triple integrator	s^3	3-D DR nav., 3-D survey route
SI + unst. mode	$s(s^2 - \eta^2)$	Bicycle/unicycle, cart w. inv. pend.
DI + lag	$s^2(s \pm p)$	Lat. motion truck w. trailer – fwd./bkwd.
Lag + stbl. mode	$(s + p)(s^2 + \omega^2)$	S/C stable pitch with a BMW
Lag + unst. mode	$(s + p)(s^2 - \eta^2)$	S/C unstable motion with a BMW
Stbl. + unst. mode	$(s^2 + \omega^2)(s^2 - \eta^2)$	S/C insertion/stationkeeping
2 stbl. modes	$(s^2 + \omega_1^2)(s^2 + \omega_2^2)$	Double pendulum, double spring–mass
2 unst. modes	$(s^2 - \eta_1^2)(s^2 - \eta_2^2)$	Double inv. pendulum
DI + double lag	$s^2(s \pm p_1)(s \pm p_2)$	Lat. motion truck w. 2 trailers – fwd./bkwd.
DI + stbl. mode	$s^2(s^2 + \omega^2)$	Crane, cart w. pend., INS, flex. robot arm
DI + unst. mode	$s^2(s^2 - \eta^2)$	Unicycle/bicycle turn, pos. cart w. inv. pend., vertical INS, ball rolling on cylinder
2 damped modes	$(s^2 + 2\zeta_1\omega_1 s + \omega_1^2)(s^2 + 2\zeta_2\omega_2 s + \omega_2^2)$	A/C longit. cruise/climb
2 lags/dpd. mode	$(s + p_1)(s + p_2)(s^2 + 2\zeta\omega s + \omega^2)$	A/C lateral cruise/turn
SI/2 dpd. modes	$s(s^2 + 2\zeta_1 s + \omega_1^2)(s^2 + 2\zeta_2\omega_2 s + \omega_2^2)$	A/C alt. dev./ landing/TO
DI/2 lags/d. mode	$s^2(s + p_1)(s + p_2)(s^2 + 2\zeta\omega s + \omega^2)$	A/C lateral path track
3 damped modes	$(s^2 + \omega_1^2)(s^2 + \omega_2^2)(s^2 + \omega_3^2)$	Trip. osc., S/C lat. w. 2 BMWs
3 unstable modes	$(s^2 - \eta_1^2)(s^2 - \eta_2^2)(s^2 - \eta_3^2)$	Trip. inv. pend., standing robot
DI/2 dpd. modes	$s^2(s^2 + \omega_1^2)(s^2 + \omega_2^2)$	Flex. S/C, cart w. double pend.
DI/2 unstable modes	$s^2(s^2 - \eta_1^2)(s^2 - \eta_2^2)$	Cart w. double inv. pend., 2 balls rolling on cylinder
DI/4 lags/ 2 damped modes	$s^2(s + p_1)(s + p_2)(s + p_3)(s + p_4) \times (s^2 + 2\zeta_1\omega_1 s + \omega_1^2)(s^2 + 2\zeta_2\omega_2 s + \omega_2^2)$	Helic. motion, landing/TO, hover pos., altitude dev.

B.2.2 Lateral Motions of a Car or Truck

The linearized lateral kinematic equations of motion for a car or truck are (see Fig. B.2)

$$\dot{\psi} = u, \qquad \dot{y} = \psi,$$

where ψ is the angle between the vehicle centerline and a reference line, y is the distance from the center of the rear axle to the reference line in units of ℓ = wheelbase (distance between the two axles), $u = \tan\delta$, and δ is the angle between the front

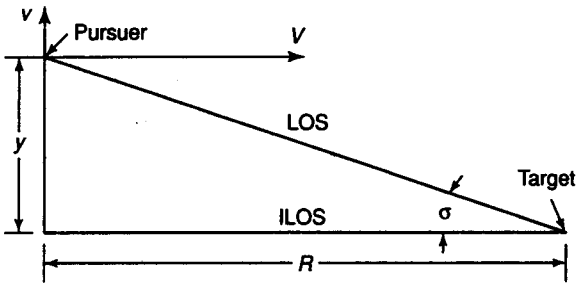

FIGURE B.1 Nomenclature for Lateral Intercept or Rendezous

wheels and the vehicle centerline. The independent variable is distance along the path in units of ℓ, i.e., time is in units of ℓ/V, where V is the velocity of the midpoint of the rear axle.

B.2.3 Lateral Motions of a Truck with a Trailer

The linearized lateral kinematic equations of motion for a three-axle vehicle such as a truck with a trailer are (see Fig. B.3)

$$\ell_1\dot{\theta}_1 = u, \qquad \ell_2\dot{\theta}_2 = \theta_1 - \theta_2, \qquad \dot{y} = \theta_1,$$

where θ_1 is the angle between the truck centerline and the reference line, θ_2 is the angle between the trailer centerline and the reference line, y is the distance from the center of the truck rear axle to the reference line, ℓ_1 is the wheelbase of the truck, ℓ_2 is the wheelbase of the trailer, $u = \tan\delta$, and δ is the angle between the truck front wheels and the truck centerline. The independent variable s is the distance along the path, i.e., $ds = V\,dt$, where V is the velocity of the midpoint of the tractor rear axle.

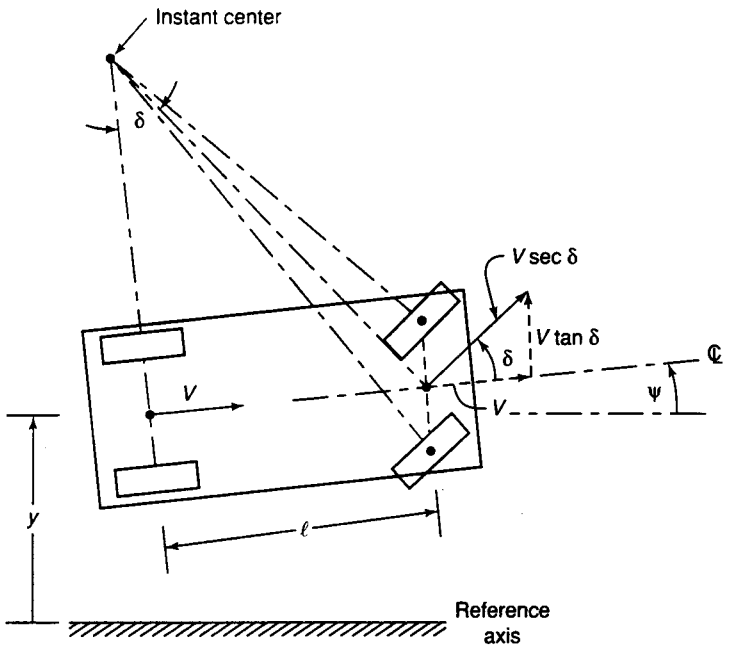

FIGURE B.2 Nomenclature for Lateral Motions of a Car or Truck

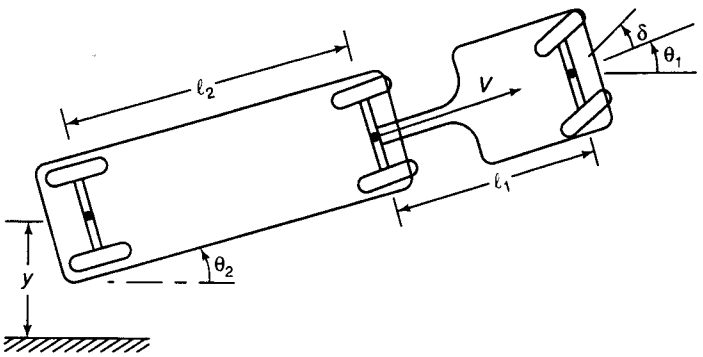

FIGURE B.3 Nomenclature for Lateral Motions of a Truck with a Trailer

For *backing up* a truck with a trailer, replace t with $-t$. This motion is unstable, so backing up is more difficult than moving forward.

B.2.4 Lateral Motions of a Truck with Two Trailers

The linearized lateral equations of motion for a four-axle vehicle such as a truck with two trailers (see Fig. B.4) are

$$\ell_1\dot{\theta}_1 = u, \quad \ell_2\dot{\theta}_2 = \theta_1 - \theta_2, \quad \ell_3\dot{\theta}_3 = \theta_2 - \theta_3, \quad \ell_4\dot{\theta}_4 = \theta_3 - \theta_4, \quad \dot{y} = \theta_4,$$

where θ_1 is the angle between the truck centerline and the reference line, θ_2 is the angle between the first trailer centerline and the reference line, θ_3 is the angle between the connecting link between the first and second trailers and the reference line, θ_4 is the angle between the second-trailer centerline and the reference line, y is the distance from the center of the second-trailer rear axle to the reference line, ℓ_1 is the wheelbase of the truck, ℓ_2 is the wheelbase of the first trailer, ℓ_3 is the length of the connecting link between the first and second trailers, ℓ_4 is the wheelbase of the second trailer, $u = \tan\delta$, and δ is the angle between the truck front wheels and the truck centerline. The independent variable s is the distance along the path, i.e., $ds = V\,dt$, where V is the velocity of the midpoint of the tractor rear axle.

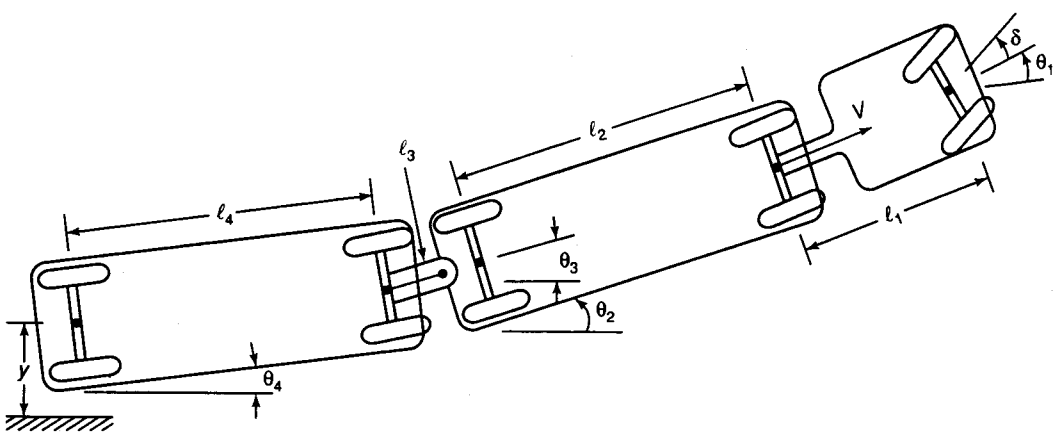

FIGURE B.4 Nomenclature for Lateral Motions of a Truck with Two Trailers

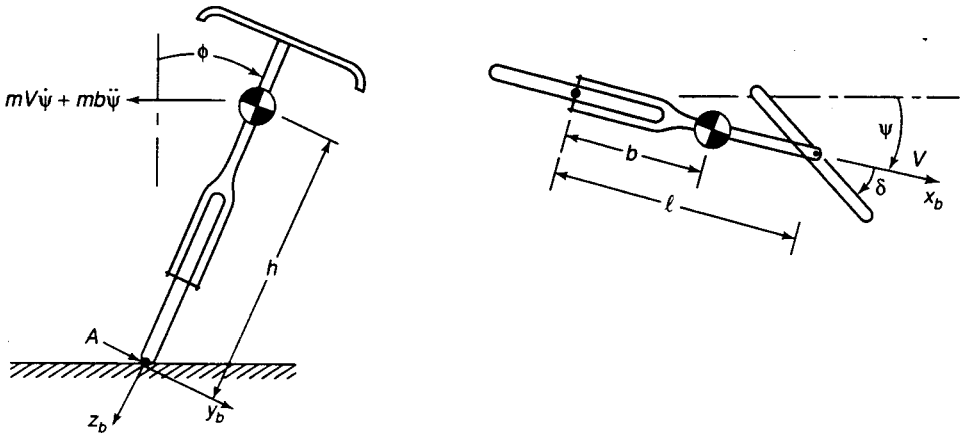

FIGURE B.5 Nomenclature for Robot Bicycle

For *backing up* a truck with two trailers, replace t with $-t$. This motion is unstable, so backing up is consierably more difficult than moving forward.

B.2.5 Bicycle Robot

A bicycle is a lateral inverted pendulum on wheels (see Fig. B.5). The linearized lateral equations of motion are

$$\ddot{\phi} = \eta^2\phi - a\delta - cu, \qquad \dot{\delta} = u, \qquad \dot{\psi} = \delta,$$

where ϕ is the roll angle from vertical, δ is the front-wheel angle away from straight ahead, u is the control, ψ is the heading angle from a reference direction, $\eta^2 = gh\ell^2/(V\rho)^2$, $a = h\ell/\rho^2$, $c = bh/\rho^2$, ℓ is the wheelbase (distance between contact points of the tires with the ground), h is the height of the center of mass of the bike plus robot above the ground, V is the forward velocity of the center of the rear wheel, g is the gravitational force per unit mass, b is the horizontal distance between the center of mass and the rear tire contact point, and ρ is the radius of gyration of the bike plus robot about the line throught the two tire contact points. The independent variable is distance along the path s in units of ℓ, i.e., $V\,dt = ds$.

If a fall begins to the right ($\phi > 0$), the rider begins to turn to the right ($\dot{\delta} \equiv u > 0$), i.e. into the direction of the fall. This yaw angular acceleration ($\ddot{\psi} \equiv u > 0$) produces a D'Alembert force $mb\ddot{\psi}$ through the mass center to the left, which opposes the fall.

In a steady turn to the right ($\dot{\psi} \equiv \delta > 0$, $\ddot{\psi}i = 0$), the centrifugal force $mV\dot{\psi}$ acts through the center of mass to the left, balancing the gravity torque $mgh\phi$ about point A. However, to start a turn to the right, the rider must first turn slightly left; this produces $\ddot{\psi} \equiv u < 0$, which tilts the bike to the right ($\ddot{\phi} > 0$) until $\eta^2\phi > 0$ is just balanced by the centrifugal force $a\dot{\psi} > 0$. To verify this behavior experimentally, ride your bike along the edge of a sidewalk curb and try to turn back onto the sidewalk – you will inevitably fall off the curb onto the street.

A typical bicycle has $\ell = 40$ in., $h = 36$ in., $b = 20$ in., $\rho \approx h$, $g = 32.2$ ft/s^2, and moves at $V = 15$ mi/h.

The TFs from the control u to ϕ and ψ are

$$\frac{\phi(s)}{u(s)} = \frac{as + c}{s(s^2 - \eta^2)}, \qquad \frac{\psi(s)}{u(s)} = \frac{1}{s^2}.$$

Hence, when using u to control both ϕ and ψ, the SRCE will have RHP *compromise* zeros (see Section 9.4).

B.2.6 Unicycle Robot

A person turns a unicycle by rotating his or her upper body about a vertical axis, which causes the unicycle wheel to rotate about a vertical axis in the opposite direction. A robot unicycle imitates this action using a reaction wheel mounted on a nominally vertical axis (whose angular velocity is nominally zero). The wheel is turned by an electric motor (see Fig. B.6). Neglecting bearing friction, the linearized equations of motion for the lateral motions of a robot unicycle are (Ref. Sw)

$$\dot{p} = \phi - Vr, \qquad \dot{\phi} = p, \qquad \dot{r} = cVp - Q, \qquad \dot{\psi} = r,$$

where ϕ is the roll angle from the vertical, p is the roll rate, r is the yaw rate, V is the forward velocity, Q is the torque applied to the reaction wheel by the motor, and ψ is the heading (yaw) angle from a reference direction. Time is in units of $1/\alpha$, where $\alpha^2 \triangleq mgh/I_x$. I_x is the moment of inertia (MOI) about the wheel–ground contact point in the forward direction of the unicycle plus rider, p, r are in units of α, Q is in units of $I_z\alpha^2$, V is in units of g/α. I_z is the MOI about a vertical axis through the ground contact point of the unicycle plus rider, m is the mass of the unicycle plus robot, h is the height of the center of mass above the ground of the unicycle plus robot, $c \triangleq (I_w/I_z)[g/(\rho\alpha^2)]$, ρ is the wheel radius, and I_w is the MOI of the reaction wheel about its axis of rotation. The product Vr is the roll torque about A due to the centrifugal force mVr acting through the center of mass. The product cVp is the gyroscopic yaw torque due to the angular momentum of the wheel and a roll rate.

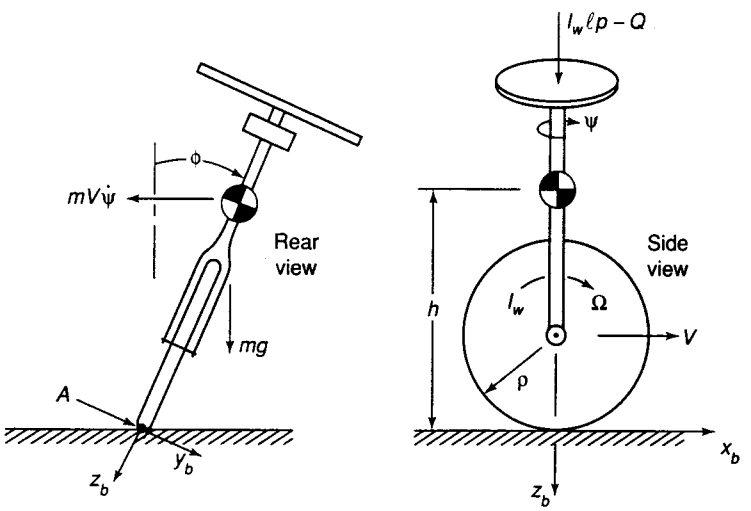

FIGURE B.6 Nomenclature for Robot Unicycle

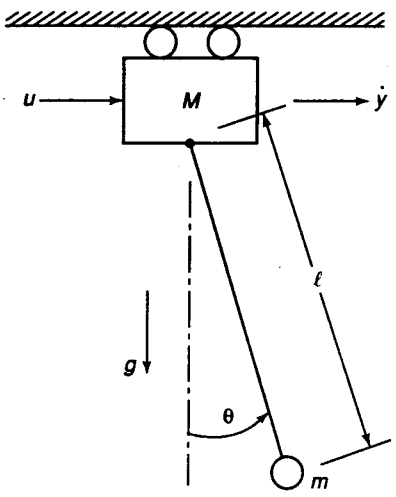

FIGURE B.7 Nomenclature for an Overhead Crane (Cart with a Pendulum)

It is straightforward to show that the plant is non-minimum-phase (NMP):

$$\frac{\phi(s)}{Q(s)} = \frac{V}{s(s^2 - 1 + cV^2)}, \qquad \frac{\psi(s)}{Q(s)} = \frac{1 - s^2}{s^2(s^2 - 1 + cV^2)}.$$

B.2.7 Overhead Crane (Cart with a Pendulum)

Figure B.7 shows an overhead crane (or cart with a pendulum), driven by an electric motor. Let ℓ be the length of the pendulum, m the mass of the load (the pendulum bob), M the mass of the cart, u the force on the cart, y the displacement of the cart, and θ the deviation of the pendulum from the vertical. The gravitational force per unit mass is g.

The equations of motion are

$$\begin{bmatrix} \dot{y} \\ \dot{v} \\ \dot{\theta} \\ \dot{q} \end{bmatrix} = \begin{bmatrix} 0 & 1 & 0 & 0 \\ 0 & 0 & \epsilon & 0 \\ 0 & 0 & 0 & 1 \\ 0 & 0 & -1 & 0 \end{bmatrix} \begin{bmatrix} y \\ v \\ \theta \\ q \end{bmatrix} + \begin{bmatrix} 0 \\ 1 \\ 0 \\ -1 \end{bmatrix} u,$$

where $\epsilon = m/(m + M)$, time is in units of $\sqrt{\ell M/g(m + M)}$, y in units of ℓ, and u in units of $(m + M)g$.

B.2.8 Cart with a Double Pendulum

The plant here is the same as in Section B.2.7, but with a double (compound) pendulum (see Fig. B.8). For the case where the two pendulum lengths are both ℓ and the two pendulum bobs and the cart each have mass m, the linearized equations of motion are

$$\dot{\theta}_1 = q_1, \qquad \dot{q}_1 = -4\theta_1 + 2\theta_2 - u, \qquad \dot{\theta}_2 = q_2, \qquad \dot{q}_2 = 2\theta_1 - 2\theta_2,$$
$$\dot{v} = 2\theta_1 + u, \qquad \dot{y} = v,$$

where time is in units of $\sqrt{\ell/g}$, y in units of ℓ, and u in units of mg.

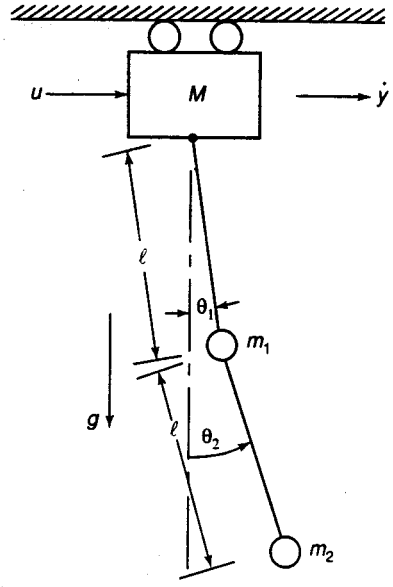

FIGURE B.8 Nomenclature for a Cart with a Double Pendulum

B.2.9 Cart with an Inverted Pendulum

Figure B.9 shows the nomenclature for a cart with an inverted pendulum. Motion of the cart can stabilize the pendulum by torquing the wheels using feedback from an angle sensor. If a (forward, backward) fall begins, the cart is (speeded up, slowed down) to maintain balance. The nomenclature and normalizations are the same as for the cart with a regular pendulum. For $|\theta| \ll 1$, the normalized equations of motion are

$$\begin{bmatrix} \dot{y} \\ \dot{v} \\ \dot{\theta} \\ \dot{q} \end{bmatrix} = \begin{bmatrix} 0 & 1 & 0 & 0 \\ 0 & 0 & -\epsilon & 0 \\ 0 & 0 & 0 & 1 \\ 0 & 0 & 1 & 0 \end{bmatrix} \begin{bmatrix} y \\ v \\ \theta \\ q \end{bmatrix} + \begin{bmatrix} 0 \\ 1 \\ 0 \\ -1 \end{bmatrix} u.$$

Note that these equations of motion are the same as those for the longitudinal motions of a robot unicycle.

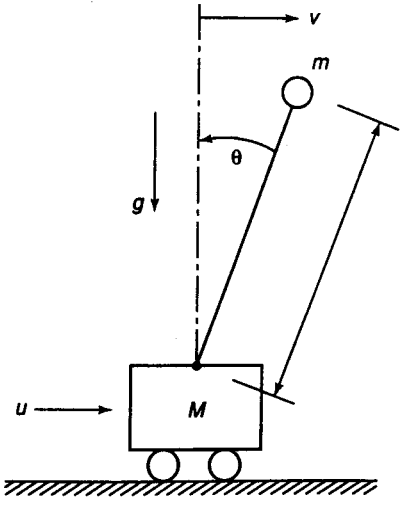

FIGURE B.9 Nomenclature for Cart with an Inverted Pendulum

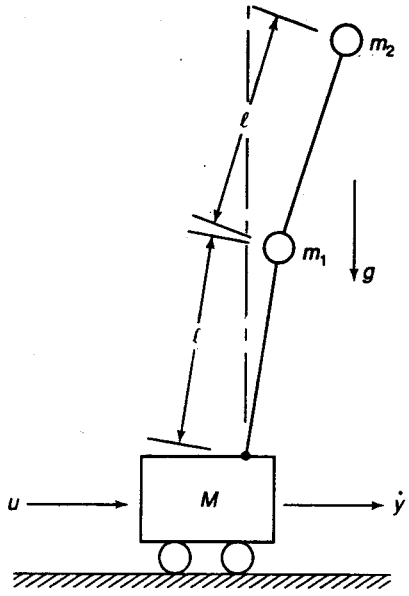

FIGURE B.10 Nomenclature for Cart with a Double Inverted Pendulum

B.2.10 Cart with a Double Inverted Pendulum

The plant here is the same as in Section B.2.9, but with a double (compound) inverted pendulum (see Fig. B.10). For the case where the two pendulum lengths are both ℓ and the two pendulum bobs and the cart each have mass m, the linearized equations of motion are

$$\dot{\theta}_1 = q_1, \qquad \dot{q}_1 = 4\theta_1 - 2\theta_2 - u, \qquad \dot{\theta}_2 = q_2, \qquad \dot{q}_2 = -2\theta_1 + 2\theta_2,$$
$$\dot{v} = -2\theta_1 + u, \qquad \dot{y} = v,$$

where time is in units of $\sqrt{\ell/g}$, y in units of ℓ, and u in units of mg.

B.2.11 Flexible Robot Arm

Figure B.11 shows a flexible robot arm (Ref. Sc). We model it using the rigid-body mode and the first bending mode, whose frequency is ω:

$$\ddot{\theta} = Q, \qquad \ddot{\delta} = -\omega^2\delta - bQ,$$

where θ is the angle of the RB mode centerline from a reference line, δ is the deflection of the tip away from the rigid-body centerline, Q is the torque at the shoulder, and b is a constant. We assume the deflection at a distance x from the shoulder is $(x/\ell)^2\delta$,

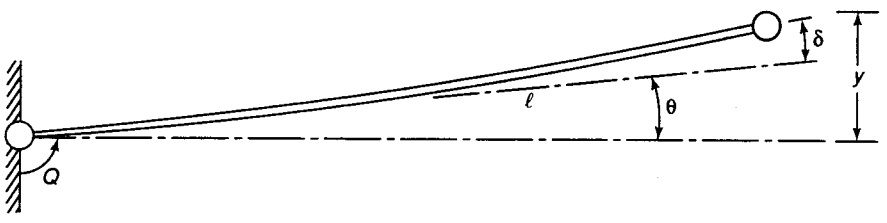

FIGURE B.11 Nomenclature for a Simplified Model of a Flexible Robot Arm

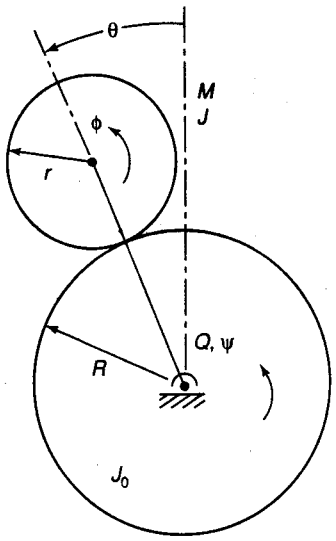

FIGURE B.12 Planetary Gear Rolling around a Rotating Sun Gear

where ℓ is the length of the arm. We wish to control the tip deflection $y = \ell\theta + \delta$ using Q.

B.2.12 Planetary Gear Rolling on a Sun Gear

Figure B.12 shows a planetary gear (PG) that is free to roll around a sun gear (SG). A link connects the center of the PG to the center of the SG (suggested by Prof. Stephen M. Rock's laboratory experiment of a ball rolling on a disk, 1999). Let R be the radius of the SG, whose center is fixed, r be the radius of the PG, ϕ be the inertial turn angle of the PG, ψ be the inertial turn angle of the SG, $(m,\ J)$ be the (mass, MOI) of the PG, J_0 be the MOI of the SG, θ be the angle of the PG from vertical, and Q be the torque applied to the SG (the control).

The equations of motion are $(R+1)\theta = \phi + R\psi$, and

$$(J+1)\ddot{\phi} + R\ddot{\psi} - \phi - R\psi = 0,$$
$$(J_0 + R^2)\ddot{\psi} + R\ddot{\phi} - R\phi - R^2\psi = Q,$$

where R is in units of r; J and J_0 in units of mr^2; time in units of $\sqrt{(R+r)/g}$; and Q in units of $mgrR/(R+r)$. The transfer function from $Q(s)$ to $\phi(s)$ is

$$\frac{\phi(s)}{Q(s)} = \frac{-c(s^2-1)}{s^2(s^2-\sigma^2)},$$

where

$$c = \frac{R}{R^2J + J_0 + JJ_0}, \qquad \sigma^2 = \frac{R^2J + J_0}{R^2J + J_0 + JJ_0} < 1.$$

The two open-loop modes at $s = 0$ correspond to $\phi + R\psi = 0$ and $\dot{\phi} + R\dot{\psi} = 0$.

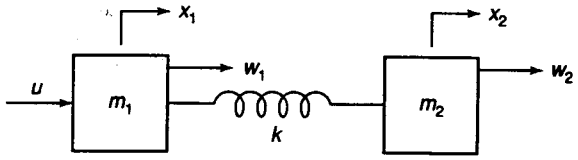

FIGURE B.13 Nomenclature for a Two-Mass–Spring Plant

B.2.13 Two-Mass–Spring Plant (Generic Flexible Space Structure)

Consider a simplified model of a flexible space structure consisting of two masses connected by a spring (see Fig. B.13). The plant model is

$$\dot{x}_1 = v_1, \qquad m\dot{v}_1 = -k(x_1 - x_2) + u + w_1, \qquad \dot{x}_2 = v_2,$$
$$m\dot{v}_2 = -k(x_2 - x_1) + w_2;,$$

where m is the mass of each body, $(x_1,\ x_2)$ are the displacements of the (left, right) body, $(v_1,\ v_2)$ are the velocities of the (left, right) body, k is the spring constant, u is the control force, and $(w_1,\ w_2)$ are disturbance forces on the (left, right) body. If we use x_i in units of a characteristic length ℓ, time in units of $\sqrt{m/k}$, and $(u,\ w)$ in units of $k\ell$, then we may put $m = 1$ and $k = 1$ in these equations of motion.

B.2.14 Standing Robot (Triple Inverted Pendulum)

A standing stick-person robot is modeled as a triple inverted pendulum with torquers at the ankle, knee, and hip joints (see Fig. B.14). The segments correspond roughly to the lower legs, thighs, and torso of a person. Just to stand still, the robot must actively stabilize using the joint torques. For the case where each segment is modeled as a rod of mass m and length ℓ, the equations of motion are (Ref. ZARBH)

$$J\ddot{\Theta} = K\Theta + BQ.$$

where $\Theta \triangleq [\theta_1\ \theta_2\ \theta_3]^T$ comprises the angular deviations from vertical of the lower

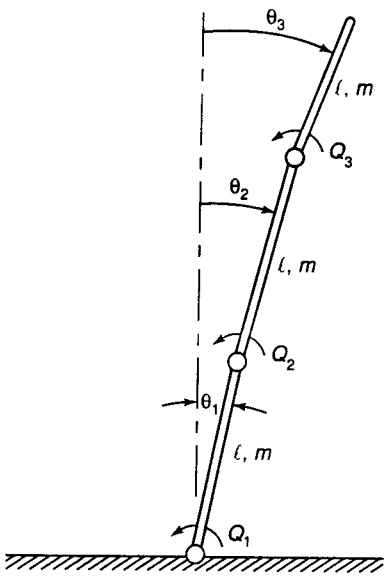

FIGURE B.14 Stick-Person Robot (Triple Inverted Pendulum)

legs, thighs, and torso, and $Q \triangleq [Q_1\ Q_2\ Q_3]^T$ comprises the torques at the ankle, knee, and hip. Using time in units of $\sqrt{\ell/g}$, J in $m\ell^2$, and K in $mg\ell$, the coefficient matrices are

$$J = J_1 + C_1 D_1, \qquad K = \frac{1}{2}\begin{bmatrix} 5 & 0 & 0 \\ 0 & 3 & 0 \\ 0 & 0 & 1 \end{bmatrix}, \qquad B = \begin{bmatrix} 1 & -1 & 0 \\ 0 & 1 & -1 \\ 0 & 0 & 1 \end{bmatrix},$$

and

$$J_1 = \frac{1}{12}\begin{bmatrix} 1 & 0 & 0 \\ 0 & 1 & 0 \\ 0 & 0 & 1 \end{bmatrix}, \qquad C_1 = \frac{1}{2}\begin{bmatrix} 1 & 2 & 2 \\ 0 & 1 & 2 \\ 0 & 0 & 2 \end{bmatrix}, \qquad D_1 = \frac{1}{2}\begin{bmatrix} 1 & 0 & 0 \\ 2 & 1 & 0 \\ 4 & 2 & 1 \end{bmatrix}.$$

B.3 Aircraft and Helicopters

B.3.1 INS Platform Tilt

Figure B.15 shows an inertial navigation system (INS) moving eastward along the equator. It consists of a platform that can be rotated with respect to the vehicle carrying it. The signal z_ϕ from a rate gyro mounted on the platform is used to rotate the platform so as to keep it (nominally) locally horizontal ($\phi = 0$). The signal z_a from an accelerometer mounted on the platform is integrated to give the vehicle velocity v. The *error* equations are (see e.g. Ref. Br2, pp. 173–175)

$$\dot{x} = v, \qquad \dot{v} = \phi, \qquad \dot{\phi} = -v + \epsilon, \qquad \dot{\epsilon} + \epsilon/\tau = w,$$

where x is the longitude error, v is the eastward velocity error, ϕ is the platform tilt angle about the north axis away from the local horizontal, ϵ is the north gyro drift, and w is a gaussian white-noise process with spectral density W. x is in units of thousandths of the earth radius ($R/1000$) (i.e. milliradians of longitude); v is in thousandths of the low-earth-orbit velocity ($\sqrt{gR}/1000$); g is the gravitational force per unit mass; time is in units of $1/\omega$, where $\omega = \sqrt{g/R}$ is the Schuler frequency; ϕ is in milliradians, and ϵ is in units of $\omega/1000$.

B.3.2 Aircraft Longitudinal Motions – Navion

The linearized longitudinal equations of motion for a general-aviation aircraft (the Navion – see Fig. B.16) flying in cruise condition (176 ft/s) near sea level are (Ref. Te)

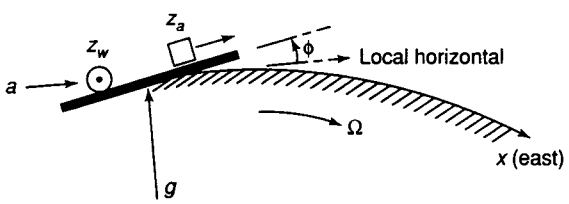

FIGURE B.15 Nomenclature for an Inertial Navigation System

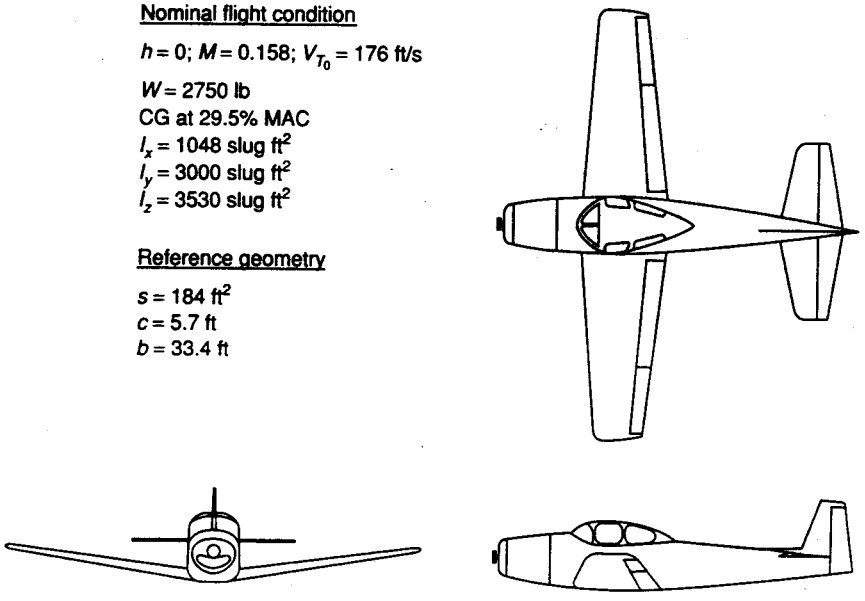

FIGURE B.16 The Navion – a General-Aviation Aircraft (Ref. Te)

$\dot{x} = Ax + B_u\delta + B_w[u_w \;\; w_w]^T$, where

$$A = \begin{bmatrix} -0.045 & 0.036 & 0 & -0.322 \\ -0.370 & -2.02 & 1.76 & 0 \\ 0.191 & -3.96 & -2.98 & 0 \\ 0 & 0 & 1 & 0 \end{bmatrix}.$$

$$B_u = \begin{bmatrix} 0 & 1 \\ -0.282 & 0 \\ -11 & 0 \\ 0 & 0 \end{bmatrix}. \qquad B_w = \begin{bmatrix} 0.045 & -0.036 \\ 0.370 & 2.02 \\ -0.191 & 3.96 \\ 0 & 0 \end{bmatrix}. \tag{B.1}$$

and the state vector is $x = [u \; w \; q \; \theta]^T$, u is the change in forward velocity, w is the change in downward velocity, θ is the pitch angle, and $q = \dot{\theta}$. The control vector is $\delta = [\delta_e \;\; \delta_T]^T$, where δ_e is the change in elevator angle and δ_T is the change in thrust specific force (proportional to throttle change). The disturbances are u_w = horizontal wind velocity and w_w = vertical wind velocity. The units are feet, seconds, and centiradians.

The altitude change h from a reference altitude and the forward displacement x from a reference point are given by $\dot{h} = -w + 1.76\theta$, $\dot{x} = u$.

B.3.3 Aircraft Lateral Motions – Navion

The linearized lateral equations of motion for a general-aviation aircraft (the Navion) flying in cruise condition (176 ft/s) near sea level are $\dot{x} = Ax + B_u\delta + B_w v_w$ (Ref. Te),

where

$$A = \begin{bmatrix} -0.254 & -1.76 & 0 & 0.322 \\ 2.55 & -0.76 & -0.35 & 0 \\ -9.08 & 2.19 & -8.4 & 0 \\ 0 & 0 & 1 & 0 \end{bmatrix},$$

$$B_u = \begin{bmatrix} 0 & 0.1246 \\ -0.222 & -4.60 \\ 29.0 & 2.55 \\ 0 & 0 \end{bmatrix}, \qquad B_w = \begin{bmatrix} 0.254 \\ -2.55 \\ 9.08 \\ 0 \end{bmatrix},$$

and the state vector is $x = [v\ r\ p\ \phi]^T$, the control vector is $\delta = [\delta_a\ \delta_r]^T$, v is the sideslip velocity, $(r,\ p)$ is the (yaw, roll) rate, ϕ is the roll angle, δ_a is the aileron angle, and δ_r is the rudder angle. The lateral specific force is $a_y = -0.254u + 0.1246\delta_r$. The disturbance is the side wind velocity v_w. The units are feet, seconds, and centiradians.

The yaw angle ψ and the lateral displacement y are given by

$$\dot{\psi} = r, \qquad \dot{y} = v + 1.76\psi.$$

B.3.4 Aircraft Longitudinal Motions – Boeing 747 at Sea Level

The linearized longitudinal equations of motion for a civil transport aircraft (the Boeing 747 – Fig. B.17, Ref. Te) flying near sea level at 221 ft/s are $\dot{x} = Ax + B_u\delta + B_w[u_w\ w_w]^T$, where

$$A = \begin{bmatrix} -0.021 & 0.122 & 0 & -0.322 & 1 \\ -0.209 & -0.530 & 2.21 & 0 & -0.044 \\ 0.017 & -0.164 & -0.412 & 0 & 0.544 \\ 0 & 0 & 1 & 0 & 0 \\ 0 & 0 & 0 & 0 & -0.25 \end{bmatrix},$$

$$B_u = \begin{bmatrix} 0.010 & 0 \\ -0.064 & 0 \\ -0.378 & 0 \\ 0 & 0 \\ 0 & 0.25 \end{bmatrix}, \qquad B_w = \begin{bmatrix} 0.021 & -0.122 \\ 0.209 & 0.530 \\ -0.017 & 0.164 \\ 0 & 0 \\ 0 & 0 \end{bmatrix},$$

and the state vector is $[u\ w\ q\ \theta\ \delta T]^T$, in which u is the perturbation in velocity along the glide slope, w is the perturbation in velocity normal to the glide slope, q is the pitch rate, θ is the perturbation in pitch angle, δT is the perturbation in thrust specific force, and u_w is the horizontal wind velocity. The control vector is $[\delta_e\ \delta_{T_c}]^T$, where δ_e is the perturbation in elevator angle, and δ_{T_c} is the perturbation in commanded thrust specific force (proportional to throttle change). The disturbances are u_w = horizontal wind velocity and w_w = vertical wind velocity. The units are feet, seconds, and centiradians.

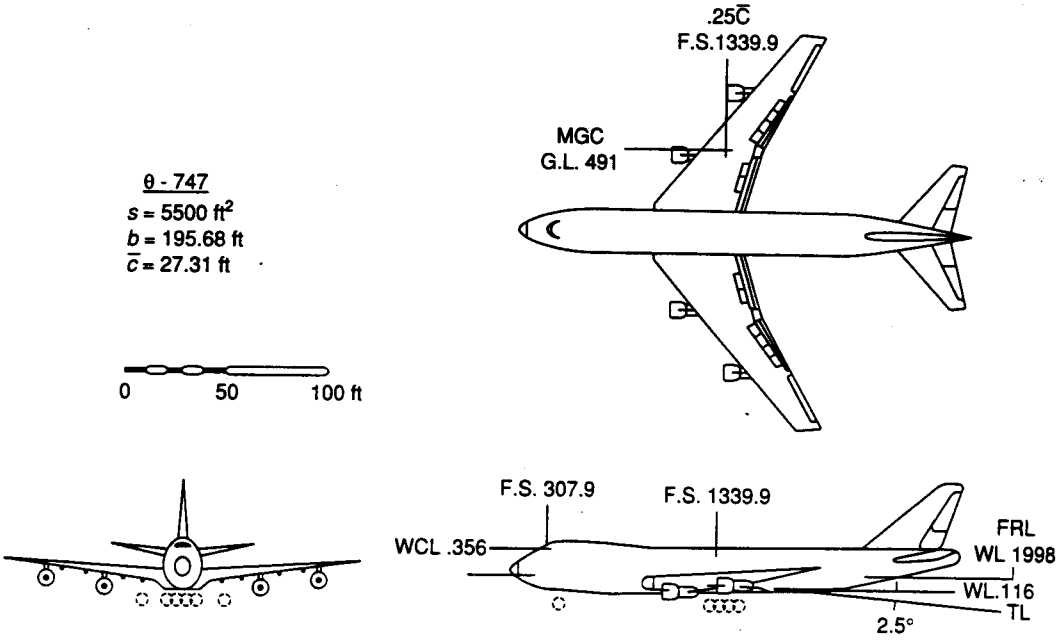

FIGURE B.17 The Boeing 747 – a Civil Transport Aircraft (Ref. HJ)

The altitude change h from a reference altitude and the forward displacement x from a reference point are given by

$$\dot{h} = -w + 2.21\theta, \qquad \dot{x} = u.$$

B.3.5 Aircraft Lateral Motions – Boeing 747 at Sea Level

The linearized lateral equations of motion for a 747 in landing configuration at sea level are (Ref. HJ) $\dot{x} = Ax + B_u\delta + B_w v_w$, where $x = [v\ r\ p\ \phi]^T$, $\delta = [\delta_a\ \delta_r]^T$, v is the lateral velocity, r is the yaw rate, p is the roll rate, ϕ is the roll angle, δ_a is the aileron angle, and δ_r is the rudder angle. The disturbance is the side wind velocity v_w. In units of feet, seconds, and centiradians, the system matrices are

$$A = \begin{bmatrix} -0.089 & -2.19 & 0 & 0.319 \\ 0.076 & -0.217 & -0.166 & 0 \\ -0.602 & 0.327 & -0.975 & 0 \\ 0 & 0.15 & 1 & 0 \end{bmatrix},$$

$$B_u = \begin{bmatrix} 0 & 0.0327 \\ 0.0264 & -0.151 \\ 0.227 & 0.0636 \\ 0 & 0 \end{bmatrix}, \qquad B_w = \begin{bmatrix} 0.089 \\ -0.076 \\ 0.602 \\ 0 \end{bmatrix}.$$

The lateral specific force is $a_y = -0.089u + 0.0327\delta_r$. The yaw angle ψ and the lateral displacement from a reference line y are given by

$$\dot{\psi} = r, \qquad \dot{y} = v + 2.19\psi.$$

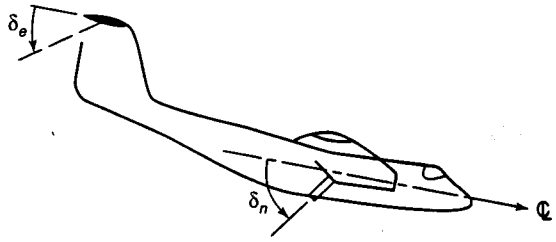

FIGURE B.18 A Short Takeoff and Landing (STOL) Aircraft

B.3.6 Aircraft Longitudinal Motions – STOL Aircraft

A STOL aircraft has a thrust nozzle that can be rotated from straight backward to directly downward (see Fig. B.18). The longitudinal equations of motion are (Ref. TB) $\dot{x} = Ax + B_u\delta + B_w[u_w \ \alpha_w]^T$ where

$$A = \begin{bmatrix} -0.0397 & -0.280 & 0 & -0.562 \\ 0.135 & -0.538 & -0.957 & 0 \\ 0.0207 & 0.441 & -1.410 & 0 \\ 0 & 0 & 1 & 0 \end{bmatrix},$$

$$B_u = \begin{bmatrix} -0.0052 & -0.102 \\ 0.031 & 0.037 \\ -1.46 & -0.066 \\ 0 & 0 \end{bmatrix}, \quad B_w = \begin{bmatrix} 0.0397 & 0.280 \\ -0.135 & 0.538 \\ 0.0207 & -0.441 \\ 0 & 0 \end{bmatrix},$$

and the state vector is $[u \ \alpha \ q \ \theta]^T$, where u is the perturbation in forward velocity, α is the angle of attack, q is the pitch rate, and θ is the pitch angle. The control vector is $\delta = [\delta_e \ \delta_n]^T$, where δ_e is the perturbation in elevator angle, and δ_n is the perturbation in nozzle angle of the deflected thrust (positive down). The altitude change h from a reference altitude and the longitudinal displacement x from a reference point are given by

$$\dot{h} = -0.0178u + 1.92\gamma, \qquad \dot{x} = u,$$

where $\gamma = \theta - \alpha$ is the flight-path angle. The disturbances are u_w = horizontal wind velocity and $\alpha_w = w_w/V$ = normalized vertical wind velocity (V = aircraft forward velocity). The units are feet, seconds, and degrees.

B.3.7 Helicopter Near Hover – OH6A

A 4I4O model of the OH6A helicopter (see Fig. B.19) takes into account the coupling between the longitudinal and lateral motions. There are four controls: δ_e = longitudinal cyclic stick, δ_c = collective stick, δ_a = lateral cyclic stick, and δ_r =

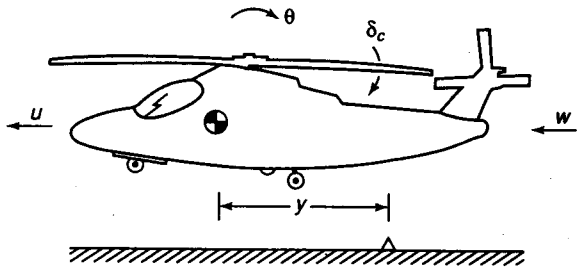

FIGURE B.19 A Medium-Size Transport Helicopter

tail-rotor collective stick. For the eight-state vector $[u\ w\ q\ \theta\ v\ r\ p\ \phi]^T$ and the control vector $\delta = [\delta_e\ \delta_c\ \delta_a\ \delta_r]$, the equations of motion near hover (Ref. He) have coefficient matrices

$$A = \begin{bmatrix} -0.0257 & 0.0113 & 0.013 & -0.3216 & 0.0004 & -0.0006 & -0.0081 & 0 \\ -0.0422 & -0.3404 & 0.0001 & -0.0093 & -0.044 & 0.0147 & 0.0005 & 0.0171 \\ 1.26 & -0.6 & -1.765 & 0 & -0.26 & 0.0719 & 0.3763 & 0 \\ 0 & 0 & 1 & 0 & 0 & 0.0532 & 0 & 0 \\ 0.0158 & -0.0194 & -0.0084 & 0 & -0.0435 & 0.0034 & -0.0134 & 0.3216 \\ -2.62 & 3.1 & -0.1724 & 0 & -0.170 & -0.8645 & -1.075 & 0 \\ 0.03 & -0.19 & -1.136 & 0 & -4.620 & -0.2873 & -4.92 & 0 \\ 0 & 0 & -0.0015 & 0 & 0 & 0.0289 & 1 & 0 \end{bmatrix},$$

$$B_u = \begin{bmatrix} 0.086 & 0.0216 & -0.0028 & -0.003 \\ -0.0016 & -0.734 & 0.0011 & -0.003 \\ -7.41 & -0.785 & 0.35 & -0.096 \\ 0 & 0 & 0 & 0 \\ -0.0038 & 0.0057 & 0.0514 & 0.153 \\ 0.493 & 9.507 & 1.982 & -25.68 \\ 1.874 & 1.206 & 12.79 & -0.781 \\ 0 & 0 & 0 & 0 \end{bmatrix}, \qquad B_w = \begin{bmatrix} 0.0257 & -.0113 & 0.0004 \\ 0.0422 & 0.3404 & 0.044 \\ -1.26 & 0.6 & 0.26 \\ 0 & 0 & 0 \\ -0.0158 & 0.0194 & 0.0435 \\ 2.62 & -3.1 & 0.170 \\ -0.03 & 0.19 & 4.670 \\ 0 & 0 & 0 \end{bmatrix},$$

where the units are feet, seconds, and centiradians for the states, and deci-inches for the controls. The disturbances are u_w = horizontal wind velocity, w_w = vertical wind velocity, and v_w = side wind velocity. The additional four kinematic states $[\psi\ x\ y\ h]^T$ are related to the eight states as follows:

$$\dot{\psi} = r, \qquad \dot{x} = u, \qquad \dot{y} = v, \qquad \dot{h} = -w,$$

where ψ is the yaw angle, $(x,\ y)$ are the horizontal coordinates of the center of mass, and h is the altitude.

Approximate 2I2O longitudinal and lateral models are obtained by neglecting the coupling between $[u, w, q, \theta; \delta_e, \delta_c; u_w, w_w]$ and $[v, p, r, \phi; \delta_a, \delta_r; v_w]$. Even simpler SISO models are obtained by further neglecting the coupling between $[u, q, \theta;\ \delta_e;\ u_w]$ and $[w;\ \delta_c;\ w_w]$, and between $[r, p, \phi;\ \delta_a]$ and $[v;\ \delta_r;\ v_w]$.

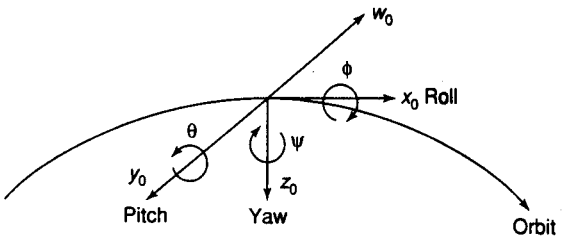

FIGURE B.20 Nomenclature for Orbital Gyrocompassing

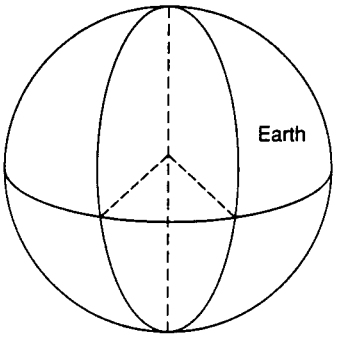

B.4 Spacecraft

B.4.1 Spacecraft Roll–Yaw Estimation (Orbital Gyrocompassing)

A spacecraft is in circular orbit with orbit rate ω (see Fig. B.20). The linearized lateral kinematic equations are

$$\dot{\phi} = \omega\psi + p, \qquad \dot{\psi} = -\omega\phi + r.$$

where ϕ is the roll angle (about the body axis nominally pointing in the direction of the orbital velocity), ψ is the yaw angle (about the body axis nominally pointing down), p is the inertial roll rate, and r is the inertial yaw rate. An horizon sensor measures the roll angle

$$y_{s\phi} = \phi + v_\phi.$$

and two rate gyros measure the roll rate and yaw rate,

$$y_{sp} = p + v_p, \qquad y_{sr} = r + v_r.$$

Treat the latter two signals as disturbance inputs in the kinematic equations, and treat the horizon sensor signal as the measurement (Ref. BK). If $(p,\ r)$ are measured in units of ω and time in $1/\omega$, then ω may be replaced by unity in the relations above.

B.4.2 Spacecraft Pitch Control Using a Reaction Wheel and Gravity Gradient

A spacecraft in circular orbit has its long axis in the flight direction, an unstable attitude due to the gravity gradient torque. By torquing a reaction wheel (RW), the spacecraft pitch angle θ can be rapidly brought close to zero (see Fig. B.21), and the RW angular velocity and θ can then be slowly reduced to zero using the gravity

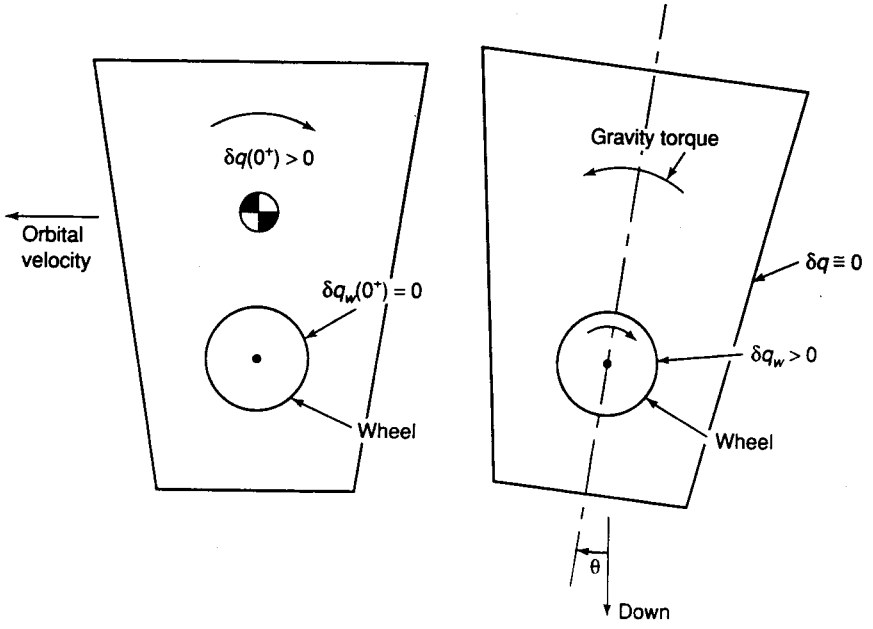

FIGURE B.21 Nomenclature for Spacecraft Pitch Control Using a Reaction Wheel and Gravity Gradient

gradient torque. The equations of motion are

$$\dot{\theta} = \delta q, \qquad \dot{\delta H} = \theta + T_d, \qquad \dot{\delta q} = \theta + T_d - \sigma\,\delta q + \frac{\sigma\,\delta H}{1+\epsilon} + e,$$

where θ is the spacecraft pitch angle relative to local horizontal, δH is the angular momentum perturbation of spacecraft plus RW from nominal equilibrium, and δq is the spacecraft pitch angular velocity perturbation. δq is in units of μ, where $\mu^2\theta$ is the destabilizing gravity-gradient angular acceleration; H is in units of $I_y\mu$, where I_y is the pitch MOI of the spacecraft plus RW; $\epsilon = J/I_y$, where J is the MOI of the RW; $\sigma \triangleq (c + N^2/R)(I_y + J)/(I_y J\mu)$, where the friction torque between the spacecraft and the RW is $c(q - q_w)$, with q_w the angular velocity of the RW in units of μ; R is the armature resistance of the RW electric motor; N is the torque per unit current in the armature; T_d is the external disturbance torque in units of $I_y\mu^2$; and e is the voltage across the armature (the control) in units of $RI_y\mu^2/N$.

B.4.3 Spacecraft Pitch Control Using a BMW and Gravity Gradient

This is the same as the model above except that the control is a bias momentum wheel (BMW), also called a control moment gyro (CMG). Torque from the spacecraft precesses the BMW away from its nominal position (angle α), and the equal and opposite torque on the spacecraft changes the spacecraft pitch angle θ. The BMW has a spin angular momentum h, and its spin axis is nominally in the flight direction (see Fig. B.22); it is free to rotate about the nominally vertical z-axis (angle α), and a control torque T can be applied to it about this axis from the spacecraft. The

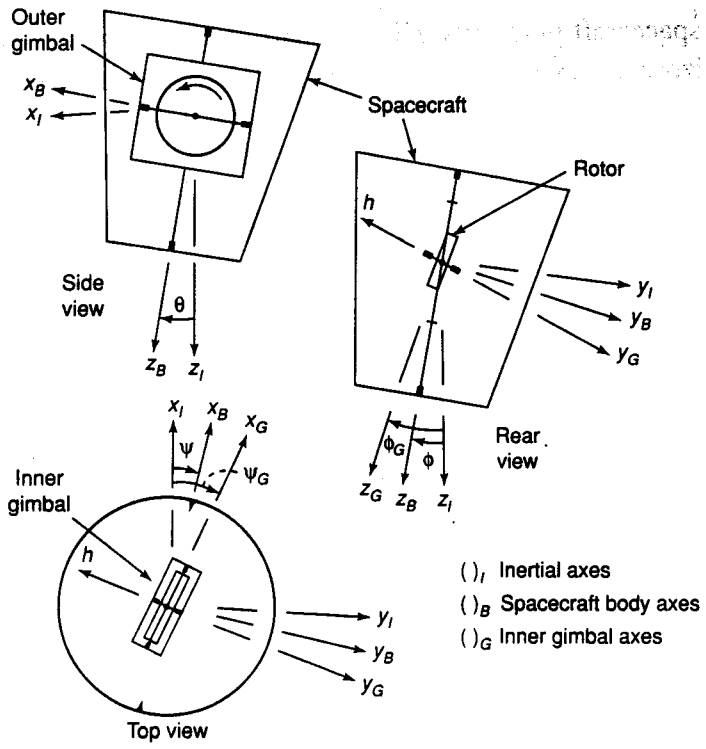

FIGURE B.22 Spacecraft with a Bias Momentum Wheel (Control Moment Gyro)

normalized equations of motion for small θ and α are

$$\ddot{\theta} = \theta - \epsilon\omega\dot{\alpha}, \qquad \ddot{\alpha} = \frac{\omega}{\epsilon}\dot{\theta} + \omega^2 T,$$

where $\omega = h/\sqrt{I_y J}$ is the nutation frequency; $\mu = n\sqrt{3(I_z - I_x)/I_y}$ is the libration reciprocal time constant; $\epsilon = \sqrt{J/I_y}$; (I_x, I_y, I_z) are the principal moments of inertia of the spacecraft plus BMW about the (roll, pitch, yaw) axes; J is the moment of inertia of the BMW about its vertical axis; and n is the orbit rate. Units are T in $J\omega^2$, t in $1/\mu$, ω in μ.

B.4.4 Spacecraft Roll–Yaw Control Using RWs and Gravity Gradient

A spacecraft in a circular orbit has its long axis (y-axis) horizontal and perpendicular to the flight direction, an unstable attitude due to the gravity gradient torque. The y-axis is also an axis of axial symmetry. By torquing roll and yaw reaction wheels (RWs) the spacecraft roll and yaw angles ϕ and ψ can be rapidly brought close to zero, and the RW angular velocities, ϕ, and ψ can then be slowly reduced to zero using the roll gravity gradient torque. The equations of motion are

$$\dot{H}_x = -ar - 3a\phi, \qquad \dot{H}_z = ap, \qquad \dot{p} = \sigma\dot{H}_x - \sigma p - ar - 3a\phi + e_x,$$
$$\dot{r} = \sigma\dot{H}_z + ap - \sigma r + e_z, \qquad \dot{\phi} = r + \psi, \qquad \dot{\psi} = r - \phi,$$

where the RW MOIs have been assumed very small compared to the spacecraft MOIs. H_x is the roll angular momentum of the spacecraft plus RWs, H_z is the yaw

angular momentum of the spacecraft plus RWs, p is the spacecraft roll angular velocity w. r. t. the locally horizontal axes, r is the spacecraft yaw angular velocity, and $(\phi,\ \psi)$ are the (roll, yaw) angles. Time is in units of $1/n$, where n is the orbit rate; $(H_x,\ H_z)$ are in units of nI, where I is the (roll, yaw) MOI of the spacecraft plus RWs, $a = (I_y - I)/I$, I_y is the pitch MOI of the spacecraft plus RWs, σ is the same as σ in Problem 9.2.13 except I_y is replaced by I, and $(e_x,\ e_z)$ are the control voltages applied to the armatures of the (roll, yaw) RW motors in units of RIn^2/N.

B.4.5 Spacecraft Roll–Yaw Control Using BMWs and Gravity Gradient

This is the same model as above except that the control actuators are bias momentum wheels (BMWs, or control moment gyros) (see Fig. B.22). Torques T_x, T_z from the spacecraft precess the BMWs away from their nominal positions (angles ϕ_g, ψ_g), and the equal and opposite torques on the spacecraft change the spacecraft (roll, yaw) angles ϕ, ψ. The normalized equations of motion for small ϕ and ψ are

$$\dot{p} = -ar - 3a\phi + T_x, \qquad \dot{r} = bp + T_z/I_z, \qquad \dot{\phi} = p + \psi, \qquad \dot{\psi} = r - \phi,$$
$$\dot{\phi}_g = -\psi_g/h, \qquad \dot{\psi}_g = \phi_g/h.$$

Time is in units of $1/n$ (n = orbit rate); p and r are in units of n; T_x and T_z are in units of $I_x n^2$; I_z is in units of I_x; h is in units of $I_x n$; $a = (I_y - I_z)/I_x$, $b = (I_y - I_x)/I_z$.

B.4.6 Spacecraft Stationkeeping and Acquisition with Thrusters

On the line between the earth and the moon there is a point called L_1 where a spacecraft would be in equilibrium, i.e., the gravitational pull of the moon plus the centrifugal force would equal gravitational pull of the earth (see Fig. B.23). However, it is an unstable equilbrium point, so that small thrusters operated by a feedback control system are required to stabilize a spacecraft there. If the thrusters are oriented along the earth–moon line, the linearized equations of motion in the orbit plane are

$$\ddot{x} = 2\dot{y} + (2\beta + 1)x + u, \qquad \ddot{y} = -2\dot{x} - (\beta - 1)y,$$

where $(x,\ y)$ is the distance from L_1 (parallel, perpendicular) to the earth–moon line, u is the thrust specific force, $\beta = 5.148$, time is in units of $1/n$, n is orbital frequency of the moon about the earth, and distance is in units of the distance from Earth to L_1.

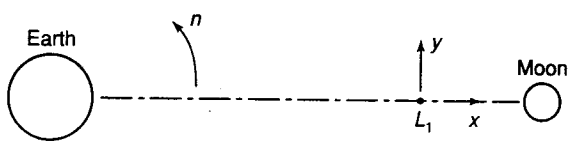

FIGURE B.23 Spacecraft Near the Earth–Moon L_1 Point

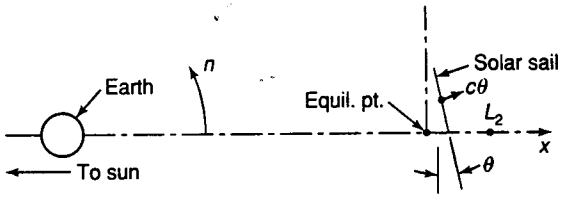

FIGURE B.24 Spacecraft with a Solar Sail Near the Sun–Earth L_2 Point

B.4.7 Spacecraft Stationkeeping and Acquisition with a Solar Sail

The sun–earth L_2 point is a point on the sun–earth line where the gravitational forces of the sun and the earth are exactly balanced by centrifugal force. A spacecraft with a large solar sail is to be placed at an equilibrium point near L_2, where the centrifugal force is augmented by the sail force (see Fig. B.24). This is an unstable equilibrium point, but the spacecraft position can be stabilized by small deviations of the sail angle θ that provide a small force perpendicular to the sun–earth line. The equations of motion, linearized about this equilbrium point, are

$$\ddot{x} = 2\dot{y} + b_1 x, \qquad \ddot{y} = -2\dot{x} - b_2 y + c\theta,$$

where (x, y) are in units of 1.51×10^6 km (the distance from earth to L_2), time is in units of $1/n$ (n = earth's angular velocity about the sun), and b_1, b_2, c are positive constants. For one spacecraft considered in a design study (S. H. Hur and B. Pervan, 1991), these constants were found to be 12.762, 4.914, 1.948, with the equilibrium point 16% closer to earth than L_2.

B.4.8 Attitude Control of a Spacecraft with Flexible Appendages

Controlling the attitude of a spacecraft with flexible appendages (see Fig. B.25) is similar to controlling a flexible robot arm (see Section B.2.11) or a two-mass–spring plant (see Section B.2.13) in that the control excites bending vibrations. A simplified model includes only one bending mode (Ref. Br2, Appendix F). Consider two sprung masses (mass m each) at a distance b from the center of mass, with spring constant k. A thruster torque $u(t)$ is used to control the pitch attitude $\theta(t)$. The linearized equations of motion have coefficients

$$A = \begin{bmatrix} 0 & 1 & 0 & 0 \\ -(1+\epsilon) & 0 & 0 & 0 \\ 0 & 0 & 0 & 1 \\ \epsilon & 0 & 0 & 0 \end{bmatrix}, \qquad B_u = \begin{bmatrix} 0 \\ -1 \\ 0 \\ 1 \end{bmatrix},$$

where $s = [y \ v \ \theta \ q]^T$, and y is the dispacement of each sprung mass from its equilibium position in units of b. Time is in units of $1/\omega$ ($\omega^2 = k/m$); $\epsilon = 2mb^2/J$, where J is the MOI of the spacecraft excluding the two sprung masses; u is in units of $J\omega^2$.

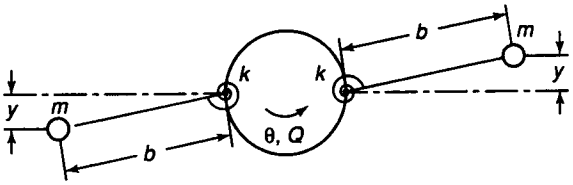

FIGURE B.25 Spacecraft with Flexible Appendages